system (ECIA). *Acta Oncol* 1993;32:853–859.
17. Garkavij M, Tennvall J, Strand S-E, et al. Extracorporeal immunoadsorption (ECIA). from whole blood based on avidin-biotin concept: evaluation of a new methodical approach. *Acta Oncol* 1996;35:309–312.
18. Zalutsky MR, Noska MA, Colapinto EV, et al. Enhanced tumor localization and in vivo stability of a monoclonal antibody radioiodinated using N-succinimydil 3-(tri-n-butylstannyl) benzoat. *Cancer Res* 1989;49:5543–5549.
19. Chen J, Strand S-E, Sjögren H-O, et al. Pharmacokinetic and biodistribution studies of paired-labeled ChiBR96 in colon carcinoma isotransplanted rat: potency of the use of extracorporeal immunoadsorption to increase the uptake ratio of tumor-to-tissue [Abstract]. *Proceedings of the Fourth Scandinavian Symposium on Radiolabeled Monoclonal Antibodies in Diagnosis and Therapy of Cancer.* Lillehammer, Sweden: 1995:7–8.
20. Norrgren K, Garkavij M, Lindgren L, et al. Evaluation of the extracorporeal immunoadsorption on the biokinetics of ^{125}I-labeled monoclonal antibody L6 in a nude rat model. *Antibody Immunoconj Radiopharm* 1994;7:29–42.
21. Siegall CB, Chase D, Mixan B, et al. In vitro and in vivo characterization of BR96sFv-PE40. A single-chain immunotoxin fusion protein that cures human breast carcinoma xenografts in athymic mice and rats. *J Immunol* 1994;3:2377–2384.
22. Stein R, Goldenberg DM, Thorpe SR, et al. Effects of radiolabeling on monoclonal antibodies with a residual iodine radiolabel on the accretion of radioisotope in tumors. *Cancer Res* 1995;55:3132–3139.
23. Khawli LA, Alauddin MM, Miller GK, et al. Improved immunotargeting of tumors with biotinylated monoclonal antibodies and radiolabeled streptavidin. *Antibody Immunoconj Radiopharm* 1993;6:13–27.
24. Isaksson M, Trail PA, Nilsson R, Helström I, Helström K-E, Sjögren HO. Use of the BR96-DOX immunoconjugate in immunotherapy against established intrahepatic tumors in an immunocompetent rat colon carcinoma model [Abstract]. In: *Proceedings of the Fifth International Conference on Anticancer Research.* Corfu, Greece: 1995:21.

Rapid Imaging of Experimental Infection with Technetium-99m-DTPA After Anti-DTPA Monoclonal Antibody Priming

Marion H.G.C. Kranenborg, Wim J.G. Oyen, Frans H.M. Corstens, Egbert Oosterwijk, Jos W.M. van der Meer and Otto C. Boerman
Departments of Nuclear Medicine, Urology and Internal Medicine, University Hospital Nijmegen, The Netherlands

Antibodies accumulate nonspecifically in infectious foci due to the locally increased vascular permeability. This study describes a method of infection imaging in which ^{99m}Tc-DTPA (diethylenetriaminepentaacetic acid) is trapped at the target by a previously administered anti-DTPA monoclonal antibody, DTIn1. **Methods:** Rats with *Staphylococcus aureus*-infected calf muscle were injected intravenously with DTIn1. Two to 24 hr after the DTIn1 injection, ^{99m}Tc-DTPA was injected intravenously. In separate experiments, excess DTIn1 was cleared from the circulation 2 hr after injection with bovine serum albumin (BSA)-DTPA-In, galactosylated BSA-DTPA-In, goat antimouse IgG or avidin. Additionally, the effect of DTIn1 dose on ^{99m}Tc-DTPA abscess uptake was determined in a three-step protocol. The distribution of the radiolabels was studied by γ counting of dissected tissue and gamma camera imaging. **Results:** Priming with DTIn1 resulted in specific retention of ^{99m}Tc-DTPA in the abscess. Such ^{99m}Tc-DTPA abscess uptake was not dependent on the interval between the DTIn1 and the ^{99m}Tc-DTPA injection: Optimal ^{99m}Tc-DTPA abscess uptake was already achieved within a 2-hr time span between the DTIn1 and DTPA injections. However, relatively high ^{99m}Tc-DTPA background was observed due to slowly clearing DTIn1-^{99m}Tc-DTPA complexes. Background reduction with various agents had a prominent effect on DTIn1 as well as ^{99m}Tc-DTPA biodistribution. The best reduction was obtained using BSA-DTPA-In. Optimal ^{99m}Tc-DTPA abscess uptake in the three-step protocol was obtained at higher DTIn1 doses (>100 μg). **Conclusion:** Infectious foci in a rat model can be imaged earlier with extremely low background levels after priming with DTIn1, followed by BSA-DTPA-In and imaging with ^{99m}Tc-DTPA, as compared with directly labeled IgG.

Key Words: technetium-99m-DTPA; monoclonal antibody priming; infection imaging; pretargeting protocols

J Nucl Med 1997; 38:901–906

Scintigraphic imaging of focal infection is currently performed with various agents, such as ^{67}Ga-citrate, radiolabeled leukocytes or ^{111}In-labeled human IgG (*1,2*). Large proteins such as IgG and human serum albumin localize nonspecifically in infectious and inflammatory foci due to the locally enhanced vascular permeability (*3,4*). Although labeled IgG is a convenient radiopharmaceutical, its relatively slow blood clearance, which causes persistently high background activity, interferes with the early diagnosis of infection and inflammation (*5*).

Reduction of background activity may be accomplished by pretargeting protocols. In these methods, the infectious focus is pretargeted and the radionuclide is administered afterwards as a low molecular weight ligand. The small ligand is rapidly excreted when not targeted to the infectious focus. Streptavidin and biotin have been used in such multistep approaches (*6–8*). Rusckowski et al. pretargeted mice with *Escherichia coli* infection with cold streptavidin and injected ^{111}In-biotin 3 hr later (*8*). Higher abscess-to-background ratios were obtained compared with ^{111}In-streptavidin or ^{111}In-IgG. Similar results were observed in tumor pretargeting studies using antichelate antibodies and radiometal labeled chelates (*9–12*).

In this study, we investigated a multistep strategy for rapid infection imaging using an anti-DTPA (diethylenetriaminepentaacetic acid) monoclonal antibody (MAb) as the pretargeting agent and ^{99m}Tc-DTPA as the targeting radiopharmaceutical.

MATERIALS AND METHODS

Radiopharmaceuticals

Technetium-99m-IgG. Human nonspecific IgG in kit form (Technescan-HIG; Mallinckrodt Medical B.V., Petten, The Netherlands) was labeled with 750 MBq ^{99m}Tc eluate according to the manufacturer's instructions.

Monoclonal Antibodies. The production of anti-DTPA MAb DTIn1 (IgG2a), reacting with DTPA loaded with different metals, has been described (*13*). The affinity constant for ^{99m}Tc-DTPA was approximately 0.2 nM^{-1}, which is similar to that for ^{111}In-DTPA (*13*). The IgG2a switch variant of MAb G250 (*14*) was used as a non-DTPA binding-control antibody. DTIn1 and G250 were labeled with ^{125}I (Amersham International, Buckinghamshire, U.K.) using the Iodogen method (*15*).

Biotinylated DTIn1. DTIn1 was conjugated with NHS-LC-biotin (Pierce, Rockford, IL). Briefly, 0.8 mg DTIn1 and 740 μg NHS-LC-biotin in 50 mM sodium phosphate (pH 7.5) were incubated for 16 hr at 4°C. Thereafter, unreacted biotin was removed by PD10 (Pharmacia LKB Technology, Uppsala, Sweden) chromatography. Each DTIn1 molecule contained 18

Received Mar. 28, 1996; accepted Aug. 12, 1996.
For correspondence or reprints contact: M.H.G.C. Kranenborg, Department of Nuclear Medicine, University Hospital Nijmegen, P.O. Box 9101, 6500 HB Nijmegen, The Netherlands.

biotins as determined by the method of Green (*16*). In vivo, the ^{99m}Tc-DTPA binding capacity of biotinylated DTIn1 and DTIn1 were similar.

Bovine Serum Albumin (BSA)-DTPA-In. BSA (Sigma Chemical Co., St. Louis, MO) was conjugated with the cyclic anhydride of DTPA (Sigma) in a 1:20 molar ratio as described by Hnatowich et al. (*17*). After PD10 chromatography to remove unreacted DTPA, excess $InCl_3$ (Merck, Darmstadt, Germany) was added. Five DTPA molecules were conjugated per BSA molecule as determined by the ITLC method described by Hnatowich et al. (*17*).

Galactosylated BSA-DTPA-In. BSA-DTPA-In was galactosylated essentially as described by Marshall et al. (*18*). To 36.5 mg dry activated galactose 10 mg BSA-DTPA-In (5 mg/ml in 25 m*M* sodium borate, pH 8.5) were added and allowed to react for 2 hr. PD10 chromatography was used to remove unreacted galactose. Thirty-two galactose molecules were conjugated per BSA-DTPA-In molecule as determined by the method of Dubois et al. (*19*).

Technetium-99m-DTPA. A kit containing 1 mg DTPA, 0.6 mg calcium nitrate and 0.05 mg stannous sulfate (pH 5.0) was radiolabeled with a fresh ^{99m}Tc eluate.

Animal Studies

Animal Model. A *Staphylococcus aureus* calf muscle abscess was induced in young, male Wistar rats according to the method of Oyen et al. (*3*). Experiments were initiated 24 hr after the *S. aureus* inoculation. All radiopharmaceuticals were intravenously injected.

Biodistribution Studies. Rats were injected intraperitoneally with a phenobarbital overdose, bled by cardiac puncture and killed. Tissues were dissected and weighed. The activity in tissues and injection standards was measured in a shielded well scintillation γ counter and expressed as the percentage of injected dose per gram (%ID/g). From these data abscess-to-blood ratios (ABR) and abscess-to-contralateral muscle ratios (AMR) were calculated. In all experiments, groups of five rats were used.

Immunoscintigraphy. Groups of four rats were anesthesized (nitrous oxide/oxygen/halothane) and placed prone on a gamma camera (Orbiter, Siemens, Hoffman Estates, IL) equipped with a low-energy, parallel hole collimator. Images (400,000 counts per image) were obtained up to 2 hr postinjection (p.i.) and stored in a 256 × 256 matrix. The images were analyzed by drawing regions of interest over the whole animal, the abscess and the contralateral calf muscle (background). The abscess-to-background ratios and abscess-to-whole body ratios were calculated.

Targeting of Infections with Technetium-99m-IgG. Each rat was injected with 25 μg ^{99m}Tc-IgG (750 MBq/mg). The rats were killed, and the biodistribution was determined 4, 8 and 24 hr after injection.

Two-Phase Targeting of Infections. Each rat was injected with 100 μg DTIn1 (3MBq/mg) or 100 μg ^{125}I-G250 (4 MBq/mg). Twenty-four hours later, the rats received 7.5 MBq ^{99m}Tc-DTPA (0.2 μg), and 2 hr later biodistribution studies were performed.

Optimization of Time Between DTIn1 and DTPA Injection. DTIn1 (100 μg labeled with 300 kBq ^{125}I) was injected into each rat. Technetium-99m-DTPA (0.2 μg labeled with 7.5 MBq) was injected at 2, 6 or 24 hr. Radiolabel biodistributions were determined 2 hr p.i.

Three-Step Targeting of Infections. Ten rats were injected with 100 μg DTIn1. Two hours later, 5 of the 10 rats received 500 μg BSA-DTPA-In. All rats received 15 MBq ^{99m}Tc-DTPA (1.4 μg) 30 min later, and images were obtained up to 120 min p.i. As control, a third group of rats received 7.5 MBq ^{99m}Tc-DTPA (0.7 μg) only. Images were obtained up to 20 min p.i.

The three-phase targeting protocol was also studied in a biodistribution experiment. Ten rats received 300 μg DTIn1 labeled with 370 kBq ^{125}I. After 2 hr, 5 of the 10 rats received 650 μg BSA-DTPA-In. Rats in both groups received 4 MBq ^{99m}Tc-DTPA (4 μg) 2.5 hr after the first injection, and biodistribution was determined 1 hr later.

Comparison of Background-Reducing Agents. Four background-reducing agents were studied in the three-step protocol: BSA-DTPA-In, galactosylated BSA-DTPA-In (gal-BSA-DTPA-In), goat antimouse IgG (GAM-IgG; rat serum absorbed; Southern Biotechnology Associates Inc., Birmingham, AL) and avidin (Sigma). Rats were injected with 30 μg DTIn1 (labeled with 2 MBq ^{125}I) or 30 μg biotinylated DTIn1 (labeled with 3 MBq ^{125}I). Two hours later, a 10-fold molar excess of background-reducing agents was injected [assuming an antibody blood level of 4%ID/g and a total blood volume of 12 ml (*3*)]. Thirty minutes later, 4 MBq ^{99m}Tc-DTPA (3.5 μg) were injected. The biodistribution was determined 30 min p.i.

Antibody Dose Optimization. Increasing amounts of ^{125}I-DTIn1 (10–900 μg per rat, labeled with 370 kBq ^{125}I) were injected. Two hours later, BSA-DTPA-In was injected into each rat at a calculated 10-fold molar excess. Thirty minutes later, each rat was injected with 4 MBq ^{99m}Tc-DTPA (3.3 μg), and ^{99m}Tc-DTPA biodistribution was determined 1 hr p.i.

Statistical Analysis. All mean values are ± s.d. Statistical analysis was performed using one-way analysis of variance, with Bonferroni post-test correction for multiple comparisons.

RESULTS

Two-Phase Targeting of Infections

Priming rats with DTIn1 for 24 hr had a profound effect on the ^{99m}Tc-DTPA biodistribution (Fig. 1). Whereas almost no differences in the biodistribution between DTIn1 and G250 were observed (data not shown), ^{99m}Tc-DTPA activity was significantly higher in DTIn1 primed rats in all examined tissues with the exception of the kidneys ($p < 0.0001$).

Optimization of the Time Between DTIn1 and DTPA Injection

In Table 1, biodistribution of ^{125}I-DTIn1 is shown 4, 8 and 26 hr after injection. The %ID/g ^{125}I-DTIn1 in the blood decreased with time. More importantly, the ^{125}I-DTIn1 uptake in the abscess was similar up to 26 hr after injection. Neither the ABR nor the AMR of ^{125}I-DTIn1 improved with time.

The %ID/g ^{99m}Tc-DTPA in blood decreased significantly with increasing intervals between the DTIn1 and DTPA injections (Table 1). The ^{99m}Tc-DTPA uptake in other organs and in the abscess was not significantly affected by the interval between the DTIn1 and ^{99m}Tc-DTPA injections. The ABR slightly improved from 0.27 at the 6-hr interval to 0.46 at the 24-hr interval between the DTIn1 and ^{99m}Tc-DTPA injections. No significant differences were observed in ^{99m}Tc-DTPA AMRs. Optimal abscess uptake of ^{99m}Tc-DTPA had been achieved during the 2 hr between the DTIn1 and DTPA injections. However, due to the high DTIn1 blood levels, ^{99m}Tc-DTPA background levels remained high.

To clarify the role of the two-step strategy, biodistribution studies with ^{99m}Tc-IgG were performed (Table 2). High background levels were also observed with ^{99m}Tc-IgG. The AMR was significantly higher using ^{99m}Tc-IgG, but no significant differences were observed in ABRs when ^{99m}Tc-IgG 4 hr post- infection was compared with ^{99m}Tc-DTPA in the two-phase protocol with a 2-hr timespan. Early imaging of infectious foci, in terms of ABRs, was not improved using this two-step protocol.

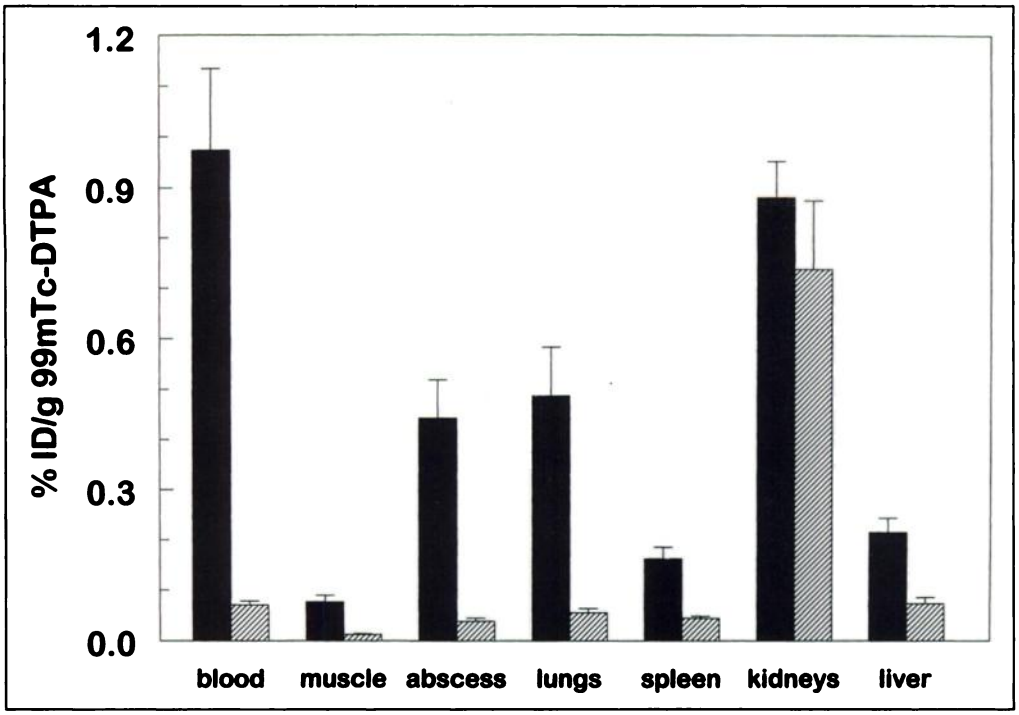

FIGURE 1. Biodistribution of ^{99m}Tc-DTPA after DTIn1 (solid bars) or G250 (hatched bars) priming. Twenty-four hours after antibody injection, rats were injected with ^{99m}Tc-DTPA, and ^{99m}Tc-DTPA biodistribution was determined 2 hr later.

Three-Step Targeting of Infectious Foci

The effect of BSA-DTPA-In on ^{99m}Tc-DTPA abscess uptake and whole-body distribution was studied scintigraphically. Administration of BSA-DTPA-In resulted in a marked change in whole-body distribution of ^{99m}Tc-DTPA (Fig. 2). With the two- and three-step protocols, the abscesses were clearly visualized. However, a notable decrease of circulating ^{99m}Tc-DTPA was observed in BSA-DTPA-In-treated rats. With the three-step protocol, the abscess-to-background ratio increased to 14.8 ± 3.1 2 hr after ^{99m}Tc-DTPA injection. Due to the rapid excretion of the nontargeted ^{99m}Tc-DTPA, the abscess uptake as a percentage of residual activity increased up to 16.3% 2 hr after ^{99m}Tc-DTPA injection. In contrast, rats receiving ^{99m}Tc-DTPA only showed minimal abscess uptake (2.3% ± 0.3% of whole-body activity 20 min p.i.), and the abscess-to-background ratio did not exceed 2.

In the biodistribution experiment, striking differences between two- and three-step protocols were observed. A decrease in ^{99m}Tc-DTPA uptake was seen in blood (17-fold reduction), abscess (1.9-fold decrease) and other organs of rats treated with BSA-DTPA-In (Fig. 3). More importantly, the ^{99m}Tc-DTPA ABR was significantly higher in three-phase protocol rats (1.97 ± 0.42 versus 0.22 ± 0.03; $p < 0.001$), whereas the AMR was not different. The %ID/g ^{125}I-DTIn1 in blood, kidneys and lungs significantly decreased, whereas a significant increase was seen in the liver and spleen, indicating DTIn1-BSA-DTPA-In complexation and subsequent metabolization (Fig. 3 inset). The amount of ^{125}I-DTIn1 in the abscess was similar in both pretargeting protocols.

The three-step approach resulted in significant improvement of the ABR for ^{99m}Tc-IgG 4 hr p.i. (1.97 ± 0.42 versus 0.35 ± 0.05; $p < 0.0001$).

Comparison of Different Background-Reducing Agents

All agents effectively reduced the %ID/g ^{99m}Tc-DTPA in the blood (Table 3). BSA-DTPA-In had the most prominent effect on ^{99m}Tc-DTPA blood levels, with a 5.6-fold reduction compared with the two-step protocol. Only slightly (but significantly) decreased ^{99m}Tc-DTPA abscess uptake was observed after injection of BSA-DTPA-In or gal-BSA-DTPA-In. Lower ^{99m}Tc-DTPA levels were observed in the liver and spleen using BSA-DTPA-In or in the liver using gal-BSA-DTPA-In.

TABLE 1
Optimization of Time Between DTIn1 and DTPA Injection

	Biodistribution of ^{125}I-DTIn1 (%ID/g or ratio; mean values ± s.d.)			Biodistribution of ^{99m}Tc-DTPA 2 hr p.i. at different intervals between DTIn1 and DTPA injections (%ID/g or ratio; mean values ± s.d.)		
Organ	4 hr p.i.	8 hr p.i.	26 hr p.i.	2-hr interval	6-hr interval	24-hr interval
Blood	3.17 ± 0.17	2.45 ± 0.15	1.50 ± 0.21	1.72 ± 0.04	1.42 ± 0.08	0.97 ± 0.16
Muscle	0.10 ± 0.02	0.08 ± 0.01	0.10 ± 0.01	0.06 ± 0.01	0.08 ± 0.03	0.08 ± 0.01
Abscess	0.83 ± 0.22	0.88 ± 0.32	0.66 ± 0.10	0.49 ± 0.12	0.48 ± 0.10	0.44 ± 0.08
Liver	0.67 ± 0.05	0.55 ± 0.13	0.28 ± 0.03	0.39 ± 0.03	0.28 ± 0.12	0.22 ± 0.03
Kidney	0.82 ± 0.08	0.77 ± 0.12	0.43 ± 0.06	1.04 ± 0.09	1.08 ± 0.23	0.88 ± 0.07
Spleen	0.48 ± 0.04	0.47 ± 0.08	0.23 ± 0.04	0.26 ± 0.02	0.20 ± 0.09	0.16 ± 0.02
ABR	0.26 ± 0.06	0.36 ± 0.15	0.44 ± 0.07	0.28 ± 0.07	0.27 ± 0.14	0.46 ± 0.06
AMR	8.96 ± 3.07	10.26 ± 2.10	6.44 ± 0.17	7.73 ± 2.21	7.43 ± 2.27	5.83 ± 0.16

p.i. = postinjection.

TABLE 2
Biodistribution of Technetium-99m-IgG (%ID/g or ratio; mean values ± s.d.)

Organ	4 hr p.i.	8 hr p.i.	24 hr p.i.
Blood	2.32 ± 0.16	1.40 ± 0.11	0.48 ± 0.07
Muscle	0.06 ± 0.01	0.06 ± 0.01	0.04 ± 0.01
Abscess	0.80 ± 0.08	0.77 ± 0.16	0.33 ± 0.05
Liver	0.96 ± 0.19	0.76 ± 0.08	0.28 ± 0.08
Kidney	8.21 ± 1.81	10.44 ± 0.87	6.96 ± 2.66
Spleen	0.98 ± 0.08	0.75 ± 0.07	0.40 ± 0.06
ABR	0.35 ± 0.05	0.55 ± 0.08	0.69 ± 0.06
AMR	12.72 ± 2.54	13.56 ± 3.57	8.09 ± 0.55

p.i. = postinjection.

Higher ^{99m}Tc-DTPA levels were observed in the spleen after GAM-IgG injection and in the liver and spleen after avidin injection. The ^{99m}Tc-DTPA ABR significantly improved using avidin (2.7-fold), BSA-DTPA-In (3.6-fold) or GAM-IgG (3.7-fold).

After injection of avidin, gal-BSA-DTPA-In or GAM-IgG, ^{125}I-DTIn1 blood levels significantly decreased compared with the two-phase protocol (Table 3). Injection of BSA-DTPA-In did not reduce ^{125}I-DTIn1 blood levels. Elevated levels of ^{125}I-DTIn1 in liver and spleen were observed after BSA-DTPA-In, avidin or GAM-IgG injection, indicating removal of complexed DTIn1 by cells of the mononuclear phagocyte system. After gal-BSA-DTPA-In injection, ^{125}I-DTIn1 was cleared through the liver, indicating that the galactose moiety directed the gal-BSA-DTPA-In-DTIn1 complexes to the liver.

Antibody Dose Escalation Studies

The amount of DTIn1 in all organs in terms of protein mass increased linearly with increasing amounts injected DTIn1 (data not shown), indicating that saturation was not reached.

Biodistribution data for ^{99m}Tc-DTPA after priming with various doses of DTIn1 are shown in Figure 4. The %ID/g in the abscess was significantly higher at ≥300 μg compared with 100 μg (0.31 ± 0.05 versus 0.19 ± 0.01; $p < 0.05$). Consequently, the ABR and AMR significantly increased when increasing the DTIn1 dose from 100–300 μg [ABR: 0.88 ± 0.03 versus 1.79 ± 0.30 ($p < 0.05$); AMR: 5.63 ± 1.71 versus 8.79 ± 2.25 ($p < 0.05$)], indicating that 300 μg per rat was the optimal dose.

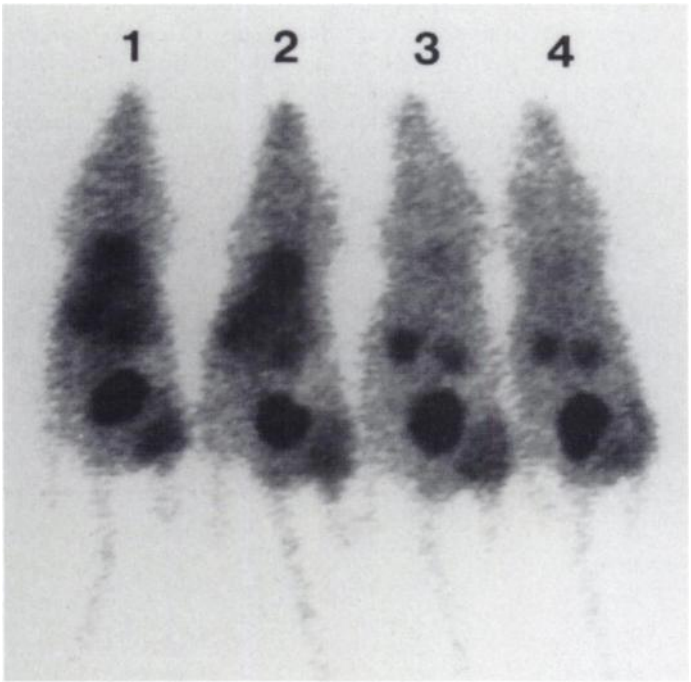

FIGURE 2. Images of rats with an *S. aureus* infection in the left calf muscle imaged at 10 min p.i. of ^{99m}Tc-DTPA using the two-phase protocol (DTIn1, ^{99m}Tc-DTPA; rats 1 and 2) or the three-phase protocol (DTIn1, BSA-DTPA-In, ^{99m}Tc-DTPA; rats 3 and 4).

DISCUSSION

The development of an imaging technique to localize acute infection within a few hours is of great clinical importance (*20*). Using radiopharmaceuticals such as ^{111}In-IgG and ^{99m}Tc-IgG a relatively long time (≥24 hr) is needed before a final diagnosis can be made (*5*). This is mainly related to slow blood clearance, resulting in slower increase of target-to-background ratios (*3*). We investigated whether a pretargeting protocol could overcome this drawback.

We evaluated the potential of an anti-DTPA MAb combined with radiolabeled DTPA for multistep targeting of infectious foci. After pretargeting with DTIn1, the abscess was visualized with ^{99m}Tc-DTPA. DTPA abscess uptake was based on antibody–antigen interaction because priming with G250 did not result in any specific ^{99m}Tc-DTPA uptake. Given the hyperemia and increased vascular permeability in acute infections, optimal abscess uptake of ^{99m}Tc-DTPA was achieved within a 2-hr time interval between the DTIn1 and DTPA injections, since accumulation of DTIn1 in the abscess was very rapid.

However, relatively high background activity was seen due to slow clearance of ^{99m}Tc-DTPA-DTIn1 complexes formed in the circulation. The two-phase protocol revealed no significant improvement in comparison to directly labeled ^{99m}Tc-IgG at early time points.

To reduce the complexation of ^{99m}Tc-DTPA with circulating DTIn1, BSA-DTPA-In was injected. This markedly changed the whole-body distribution of the subsequently injected ^{99m}Tc-DTPA. The imaging studies showed only minor amounts of ^{99m}Tc-DTPA in the circulation, whereas the abscess was clearly visualized.

Four different background-reducing agents were compared. Immune complexes formed between DTIn1 and avidin, GAM-IgG or BSA-DTPA-In should be cleared through the liver and spleen (*9,21–25*). DTIn1-Gal-BSA-DTPA-In complexes should be cleared through the hepatic asialoglycoprotein receptor (*26*). Avidin and GAM-IgG do not interfere with the antigen-binding site of DTIn1, whereas BSA-DTPA-In and gal-BSA-DTPA-In do. Each of the background-reducing agents significantly reduced the amount of ^{99m}Tc-DTPA in the blood. The enhanced ^{99m}Tc-DTPA liver and spleen uptake seen with avidin and GAM-IgG most likely represents ^{99m}Tc-DTPA entrapment by DTIn1 complexes not yet metabolized. In contrast, reduced amounts of ^{99m}Tc-DTPA were observed in the spleen and/or liver with gal-BSA-DTPA-In and BSA-DTPA-In, indicating efficient blocking of the DTPA-binding site. Significantly decreased ^{99m}Tc-DTPA abscess uptake was observed with BSA-DTPA-In and gal-BSA-DTPA-In. This reduced abscess uptake resulted from blocking of DTIn1 antibody in the abscess or blockage of circulating DTIn1 (thereby reducing the number of circulating DTIn1-DTPA complexes contributing to ^{99m}Tc-DTPA abscess uptake). These data suggest that ^{99m}Tc-DTPA binding to prelocalized DTIn1 plays an important role in ^{99m}Tc-DTPA abscess uptake, in view of the slight reduction in the amount of ^{99m}Tc-DTPA in the abscess after BSA-DTPA-In injection.

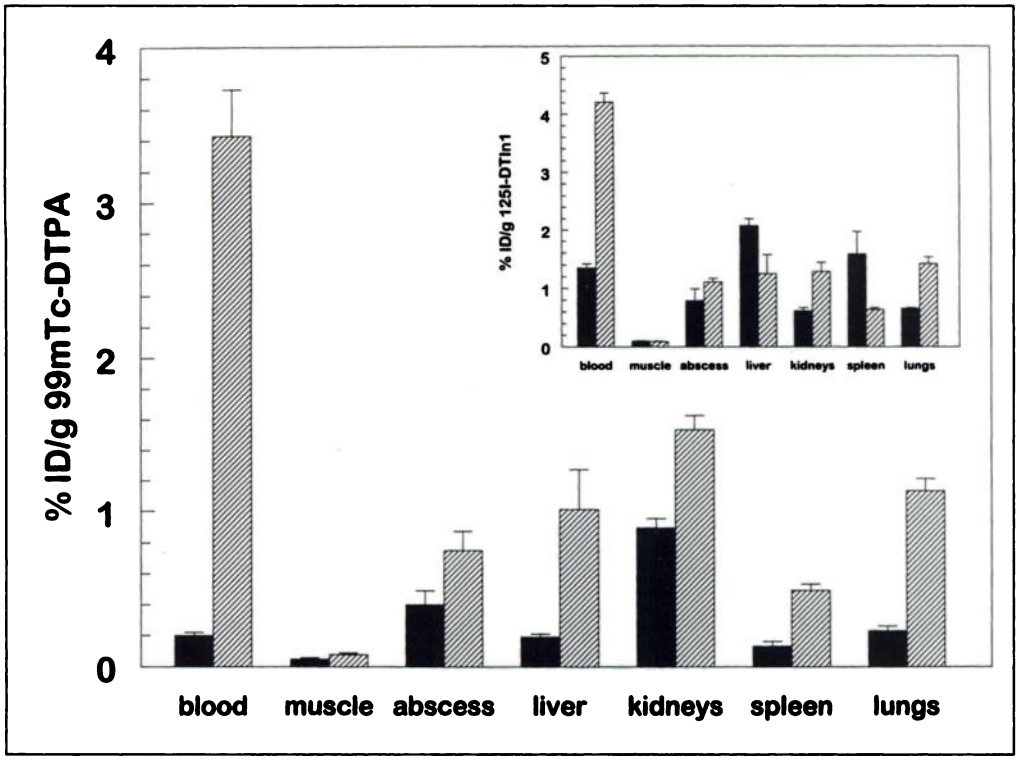

FIGURE 3. Comparison between the three-phase protocol (DTIn1, BSA-DTPA-In, DTPA; solid bars) and the two-phase protocol (DTIn1, DTPA; hatched bars). Biodistribution of ^{99m}Tc-DTPA 1 hr after injection is shown. Biodistribution of ^{125}I-DTIn1 3.5 hr after injection is shown in the inset.

The best reduction of ^{99m}Tc-DTPA background was obtained with BSA-DTPA-In: A 5.6-fold reduction of ^{99m}Tc-DTPA blood level was achieved with a concomittant 3.5-fold increase in the ABR. The use of a background-reducing agent that can block the DTIn1 antigen-binding site does not hamper the targeting of infectious foci with ^{99m}Tc-DTPA. Therefore, the behavior of BSA-DTPA-In in these studies was superior to the other background-reducing agents.

Goodwin et al. used a similar background reduction approach to image tumors in mice (*9*). A three-step protocol was designed using an anti-BLEDTA IV antibody, a human transferrin-chelate conjugate and ^{111}In-BLEDTA IV. Due to the background reduction step, decreased ^{111}In-BLEDTA IV tumor uptake and increased tumor-to-blood ratios were observed similar to our observations. In their study of mice with *E. coli* infection, Rusckowski et al. demonstrated that infection imaging could be improved, in terms of ABR and AMR, using streptavidin pretargeting and radiolabeled biotin (*8*).

With our three-step strategy, rapid imaging of infectious foci was achieved: high abscess-to-background ratios were obtained within 30 min p.i. of DTPA and 3 hr after the first injection. The three-phase targeting protocol may potentially improve the infection imaging at earlier times after tracer injection in humans. A limitation to this approach might be the development of a HAMA response after administration of DTIn1. For clinical studies, a humanized DTIn1 antibody is preferable. Immuno-

TABLE 3
Comparison of Different Background Reducing Agents

Organ	DTIn1	BSA-DTPA-In	Galactosylated BSA-DTPA-In	Goat anti-mouse IgG	Avidin
		Biodistribution of ^{125}I-DTIn1 (%ID/g; mean value ± s.d.)			
Blood	3.81 ± 0.27	3.77 ± 0.32	1.90 ± 0.10*	0.57 ± 0.06*	0.82 ± 0.09*
Muscle	0.08 ± 0.004	0.08 ± 0.01	0.07 ± 0.005	0.11 ± 0.01*	0.11 ± 0.01†
Abscess	1.00 ± 0.21	0.93 ± 0.22	0.54 ± 0.14‡	0.56 ± 0.05‡	0.59 ± 0.07†
Liver	0.68 ± 0.10	1.07 ± 0.12*	3.28 ± 0.19*	2.67 ± 0.08*	1.99 ± 0.19*
Spleen	0.65 ± 0.08	1.25 ± 0.11*	0.46 ± 0.03‡	2.63 ± 0.42*	2.71 ± 0.54*
		Biodistribution of ^{99m}Tc-DTPA (%ID/g or ratio; mean value ± s.d.)			
Blood	2.25 ± 0.20	0.40 ± 0.04*	1.16 ± 0.08*	0.51 ± 0.04*	0.72 ± 0.09*
Muscle	0.08 ± 0.003	0.07 ± 0.01	0.08 ± 0.01	0.08 ± 0.01	0.08 ± 0.01
Abscess	0.56 ± 0.11	0.36 ± 0.09†	0.39 ± 0.09†	0.47 ± 0.05	0.48 ± 0.08
Liver	0.45 ± 0.06	0.15 ± 0.02*	0.33 ± 0.03‡	0.50 ± 0.04	0.76 ± 0.06*
Spleen	0.29 ± 0.17	0.11 ± 0.01†	0.22 ± 0.01	1.78 ± 0.29*	1.34 ± 0.30*
ABR	0.25 ± 0.04	0.90 ± 0.26*	0.34 ± 0.08	0.92 ± 0.09*	0.67 ± 0.07*
AMR	7.29 ± 1.49	5.17 ± 0.86†	5.34 ± 1.57	6.06 ± 0.75	5.89 ± 1.01

*Significant difference as compared with two-phase protocol (i.e., DTIn1) at $p < 0.001$.
†Significant difference as compared with two-phase protocol at $p < 0.01$.
‡Significant difference as compared with two-phase protocol at $p < 0.001$.
No significant differences were observed between DTIn1 and biotinylated DTIn1; only DTIn1 results are shown.

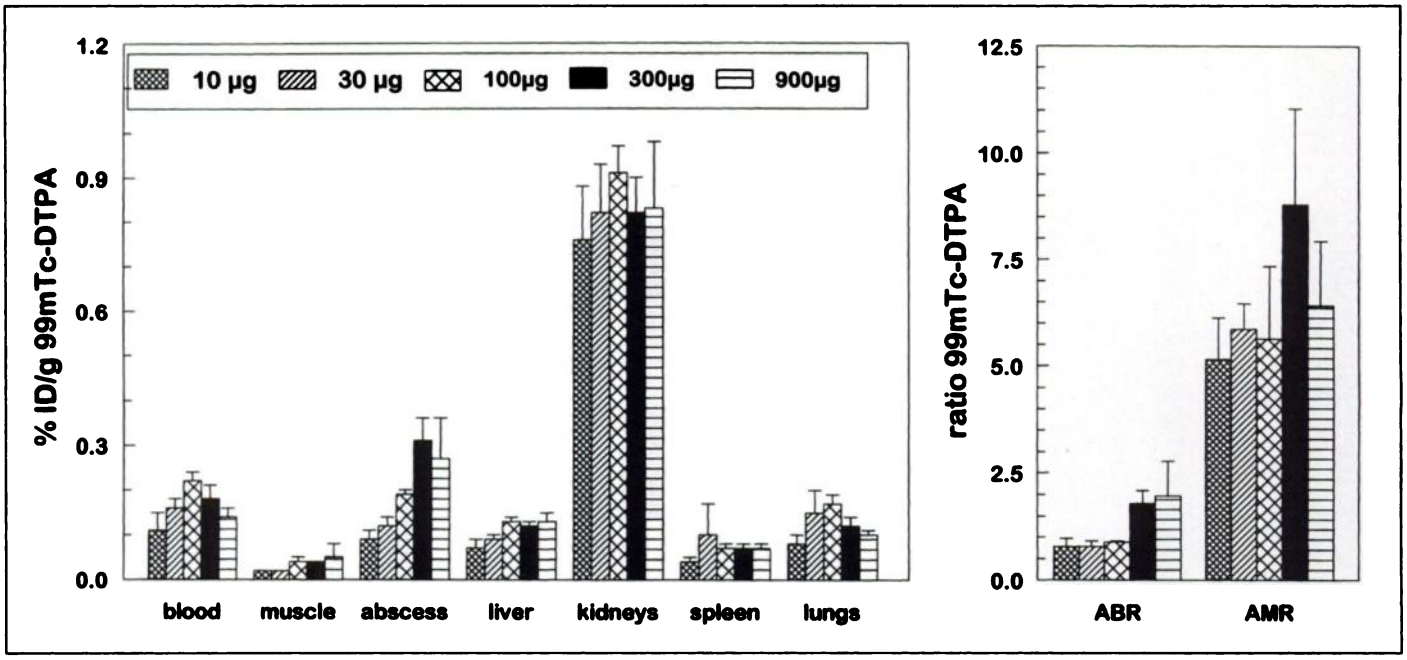

FIGURE 4. Biodistribution of ^{99m}Tc-DTPA after priming with increasing DTIn1 doses and chasing with a 10-fold molar excess of BSA-DTPA-In. Two hours after DTIn1 injection, BSA-DTPA-In was injected, and DTPA was injected 30 min later. Biodistribution data were obtained 1 hr after DTPA injection.

genicity of the background-reducing agent can be minimized by the use of a human serum protein as a carrier. The immunogenicity of avidin (*6*) might hamper the use of the avidin-biotin system for infection imaging in humans, especially since a human equivalent of avidin is not available.

A potential drawback to the three-step method is the relatively large DTIn1 protein dose needed in humans. The use of multivalent DTPA might facilitate the use of lower DTIn1 doses in view of the higher affinity of antichelate antibodies for multivalent chelates compared to monovalent chelates (*11*).

CONCLUSION

Three-phase targeting of infectious foci results in early imaging with low background levels as compared with two-phase targeting protocols or directly labeled nonspecific IgG.

ACKNOWLEDGMENTS

We thank Mrs. J.C. Oosterwijk-Wakka and Mrs. M.C.A. de Weijert (University of Nijmegen, Department of Urology), Mr. E. Koenders (University of Nijmegen, Department of Nuclear Medicine) and Mr. G. Grutters and Mr. H. Eijkholt (University of Nijmegen, Central Animal Laboratory) for technical assistance. This study was partially supported by Research Grant 93–539 from the Dutch Cancer Society.

REFERENCES

1. Rubin RH, Fischman AJ, Needleman M, et al. Radiolabeled, nonspecific, polyclonal human immunoglobulin in the detection of focal inflammation by scintigraphy: comparison with gallium-67 citrate and technetium-99m-labeled albumin. *J Nucl Med* 1989;30:385–389.
2. Oyen WJG, Claessens RAMJ, van der Meer JWM, Rubin RH, Strauss HW, Corstens FHM. Indium-111-labeled human nonspecific immunoglobulin G: a new radiopharmaceutical for imaging infectious and inflammatory foci. *Clin Infect Dis* 1992;14: 1110–1118.
3. Oyen WJG, Claessens RAMJ, van der Meer JWM, Corstens FHM. Biodistribution and kinetics of radiolabeled proteins in rats with focal infection. *J Nucl Med* 1992;33:388–394.
4. Morrel EM, Tompkins RG, Fischman AJ, et al. Autoradiographic method for quantitation of radiolabeled proteins in tissues using indium-111. *J Nucl Med* 1989;30:1538–1545.
5. Fischman AJ, Babich JW, Rubin RH. Infection imaging with technetium-99m-labeled chemotactic peptide analogs. *Semin Nucl Med* 1994;24:154–168.
6. Paganelli G, Magnani P, Zito F, et al. Three-step monoclonal antibody tumor targeting in carcinoembryonic antigen-positive patients. *Cancer Res* 1991;51:5960–5966.
7. Hnatowich DJ, Fritz B, Virzi F, Mardirossian G, Rusckowski M. Improved tumor localization with (strept)avidin and labeled biotin as a substitute for antibody. *Nucl Med Biol* 1993;20:189–195.
8. Rusckowski M, Fritz B, Hnatowich DJ. Localization of infection using streptavidin and biotin: an alternative to nonspecific polyclonal immunoglobulin. *J Nucl Med* 1992;33:1810–1815.
9. Goodwin DA, Meares CF, McCall MJ, McTigue M, Chaovapong W. Pretargeted immunoscintigraphy of murine tumors with indium-111-labeled bifunctional haptens. *J Nucl Med* 1988;29:226–234.
10. Le Doussal JM, Martin M, Gautherot E, Delaage M, Barbet J. In vitro and in vivo targeting of radiolabeled monovalent and divalent haptens with dual specificity monoclonal antibody conjugates: enhanced divalent hapten affinity for cell-bound antibody conjugate. *J Nucl Med* 1989;30:1358–1366.
11. Le Doussal JM, Gruaz-Guyon A, Martin M, et al. Targeting of indium-labeled bivalent hapten to human melanoma mediated bispecific monoclonal antibody conjugates: imaging of tumors hosted in nude mice. *Cancer Res* 1990;50:3445–3452.
12. Stickney DR, Anderson LD, Slater JB, et al. Bifunctional antibody: a binary radiopharmaceutical delivery system for imaging colorectal carcinoma. *Cancer Res* 1991;51:6650–6655.
13. Kranenborg MHGC, Boerman OC, Oosterwijk-Wakka JC, de Weijert MCA, Corstens FHM, Oosterwijk E. Development and characterization of anti-renal-cell carcinoma x anti-DTPA bispecific monoclonal antibodies for two-phase targeting of renal-cell carcinoma. *Cancer Res* 1995;55:5864S–5867S.
14. Oosterwijk E, Ruiter DJ, Hoedemaeker PJ, et al. Monoclonal antibody G250 recognizes a determinant present in renal-cell carcinoma and absent from normal kidney. *Int J Cancer* 1986;38:489–494.
15. Fraker PJ, Speck JC Jr. Protein and cell membrane iodinations with a sparingly soluble chloramide, 1,3,4,6-tetrachloro-3a,6a-diphrenylglycoluril. *Biochem Biophys Res Commun* 1978;80:849–857.
16. Green NM. A spectrophotometric assay for avidin and biotin based on binding of dyes by avidin. *Biochem J* 1965;94:23c–24c.
17. Hnatowich DJ, Childs RL, Lanteigne D, Najafi A. The preparation of DTPA-coupled antibodies radiolabeled with metallic radionuclides: an improved method. *J Immunol Methods* 1983;65:147–157.
18. Marshall D, Pedley RB, Melton RG, Boden JA, Boden R, Begent RHJ. Galactosylated streptavidin for improved clearance of biotinylated intact and $F(ab')_2$ fragments of an anti-tumor antibody. *Br J Cancer* 1995;71:18–24.
19. Dubois M, Gilles KA, Hamilton JK, Rebers PA, Smith F. Colorimetric method for determination of sugars and related substances. *Anal Chem* 1956;28:350–356.
20. Corstens FHM, van der Meer JWM. Chemotactic peptides: new locomotion for imaging of infection? *J Nucl Med* 1991;32:491–494.
21. Yao Z, Zhang M, Kobayashi H, et al. Improved targeting of radiolabeled streptavidin in tumors pretargeted with biotinylated monoclonal antibodies through an avidin chase. *J Nucl Med* 1995;36:837–841.
22. Kobayashi H, Sakahara H, Endo K, et al. Comparison of the chase effects of avidin, streptavidin, neutravidin and avidin-ferritin on a radiolabeled biotinylated anti-tumor monoclonal antibody. *Jpn J Cancer Res* 1995;86:310–314.
23. Sinitsyn VV, Mamontova AG, Checkneva YY, Shnyra AA, Domogatsky SP. Rapid blood clearance of biotinylated IgG after infusion of avidin. *J Nucl Med* 1989;30:66–69.
24. Sharkey RM, Primus FJ, Goldenberg DM. Second antibody clearance of radiolabeled antibody for cancer radioimmunodetection. *Proc Natl Acad Sci USA* 1984;81:2843–2846.
25. Sharkey RM, Mabus J, Goldenberg DM. Factors influencing anti-antibody enhancement of tumor targeting with antibodies in hamsters with human colonic tumor xenografts. *Cancer Res* 1988;48:2005–2009.
26. Stockert RJ. The asialoglycoprotein receptor: relationships between structure, function and expression. *Physiol Rev* 1995;75:591–609.